Research Journal of Applied Sciences, Engineering and Technology 1(3): 98-106, 2009
ISSN: 2040-7467

Submitted Date: May 27, 2009 Accepted Date: August 01, 2009 Published Date: October 20, 2009

MHD Heat and Mass Transfer Free Convection Flow along a Vertical Stretching Sheet in Presence of Magnetic Field with Heat Generation

M.A. Samad and M. Mohebujjaman
Department of Mathematics, Dhaka University, Dhaka-1000, Bangladesh

Abstract: The steady two-dimensional magnetohydrodynamic heat and mass transfer free convection flow of a viscous incompressible fluid near an isothermal linearly stretching sheet in the presence of a uniform magnetic field with heat generation is considered. The equations governing the flow, temperature and concentration field are reduced to a system of coupled non-linear ordinary differential equations. These non-linear differential equations are integrated numerically by using Nachtsheim-Swigert shooting iteration technique along with sixth order Runge-Kutta integration scheme. Finally the effects of the pertinent parameters which are of physical and engineering interest are examined both in graphical and tabular form.

Key words: Boundary layer, buoyancy force, electric conductivity, molecular diffusivity and Schmidt number

INTRODUCTION

Laminar boundary layer behavior over a moving continuous and linearly stretching surface is a significant type of flow has considerable practical applications in engineering, electrochemistry, D. T. Chin (1975), R. S. R. Gorla (1978) and polymer processing, R.M. Griffith (1964), L.E. Erickson *et al*., (1966). For example, materials manufactured by extrusion processes and heat-treated materials traveling between a feed roll and a wind-up roll or on a conveyor belt possess the characteristics of a moving continuous surface. The hydromagnetic flow and heat transfer problems have become important industrially. To be more specific, it may be pointed out that many metallurgical processes involve the cooling of continuous strips or filaments by drawing them through a quiescent fluid and that in the process of drawing, these strips are sometimes stretched. Mention may be made of drawing, annealing and tinning of copper wires. In all the cases the properties of the final product depend to a great extent on the rate of cooling. By drawing such strips in an electrically conducting fluid subjected to a magnetic field, the rate of cooling can be controlled and a final product of desired characteristics can be achieved. Another interesting application of hydromagnetics to metallurgy lies in the purification of molten metals from nonmetallic inclusions by the application of a magnetic field. The study of heat and mass transfer is necessary for determining the quality of the final product. However, there are fluids, which react chemically with some other ingredients present in them. The effect of a chemical reaction on the flow past an impulsively started infinite vertical plate with uniform heat flux was studied by Das *et al*., (1994). Anderson *et al*., (1994) have studied the diffusion of a chemically reactive species from a linearly stretching sheet. Anjalidevi and Kandasamy (1999) investigated the effect of a chemical reaction on the flow along a semi-infinite horizontal plate in the presence of heat transfer. Anjalidevi and Kandasamy (2000) have studied the effect of a chemical reaction on the flow in the presence of heat transfer and magnetic field. Muthucumaraswamy and Ganesan (2000) have analyzed the effect of a chemical reaction on the unsteady flow past an impulsively started semi-infinite vertical plate, which is subject to uniform heat flux. McLeod and Rajagopal (1987) have investigated the uniqueness of the flow of a Navier Stokes fluid due to a linear stretching boundary. Raptis *et al*., (2006) have studied the viscous flow over a non-linearly stretching sheet in the presence of a chemical reaction and magnetic field.

In 1961, Sakiadis (1961) who developed a numerical solution for the boundary layer flow field over a continuous solid surface moving with constant speed. Due to entrainment of ambient fluid, this boundary layer flow situation is quite different from the classical Blasius problem of boundary flow over a semi-infinite flat plate. Suction or injection of a stretched surface was studied by Erickson *et al*., (1966) and Fox *et al*., (1968) for uniform surface velocity and temperature and investigated its effects on the heat and mass transfer in the boundary layer. Chen and Char (1988) have studied the suction and injection on a linearly moving plate subject to uniform wall temperature and heat flux and the more general case using a power law velocity and temperature distribution at the surface was studied by Ali (1995). Magyari *et al*., (2001) have reported analytical and computational solutions when the surface moves with rapidly decreasing velocities using the self-similar method. In all papers mentioned above the effect of buoyancy force was relaxed.The above investigations having a definite bearing on the problem of a polymer sheet extruded continuously from a dye. It is usually assumed that the sheet is inextensible, but situations may arise in the polymer industry in which it is necessary to deal with a stretching plastic sheet, as noted by Crane (1970). The study of heat generation or absorption in moving fluids is important in problems dealing with chemical reactions and these concerned with dissociating fluids. Possible heat

Corresponding Author: M.A. Samad , Department of Mathematics, Dhaka University, Dhaka-1000, Bangladesh

generation effects may alter the temperature distribution; consequently, the particle deposition rate in nuclear reactors, electronic chips and semi conductor wafers. Vajravelu and A. Hadjinicolaou (1997) studied the heat transfer characteristics in the laminar boundary layer of a viscous fluid over a stretching sheet with viscous dissipation or frictional heating and internal heat generation.The aim of this paper is to make a numerical calculation, on convective heat and mass transfer flow which have been of interest to the engineering community and to the investigators dealing with the problem in geophysics, astrophysics, electrochemistry and polymer processing. From the technical point of view free convection flow past an infinite or semi-infinite vertical plate is always important for many practical applications. Usually in such types of flows, the thermal diffusion effect is neglected. In the present paper, we have investigated the effect of a chemical reaction of an electrically conducting viscous incompressible fluid on the flow over a linearly stretching vertical sheet in the presence of heat and mass transfer as well as a uniform magnetic field which is normal to the sheet with heat generation/absorption.

Mathematical Analysis: A steady-state two-dimensional heat and mass transfer flow of an electrically conducting viscous incompressible fluid along an isothermal stretching vertical sheet with heat generation/absorption is considered. The stretching sheet coincides with the plane y = 0 where the flow is confined to y > 0 A uniform magnetic field of strength B_0 is imposed along the y-axis. Two equal and opposite forces are introduced along the -axis so that the sheet is stretched keeping the origin fixed as shown in Fig. 1.

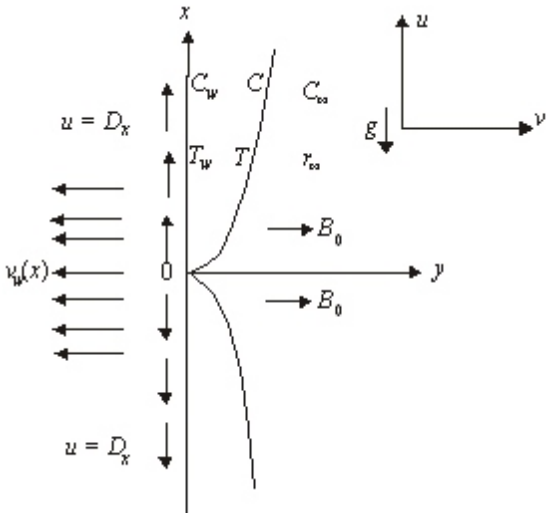

Fig 1: Flow configuration and coordinate system.

The boundary-layer equations relevant to the problem are:

$$\frac{\partial u}{\partial x} + \frac{\partial v}{\partial y} = 0 \tag{1}$$

$$u\frac{\partial u}{\partial x} + v\frac{\partial u}{\partial y} = u\frac{\partial^2 u}{\partial y^2} + sg\beta(T - T_\infty) - \frac{\sigma B_0^2 u}{\rho} \tag{2}$$

$$u\frac{\partial T}{\partial x} + v\frac{\partial T}{\partial y} = \frac{\kappa}{\rho c_p}\frac{\partial^2 T}{\partial y^2} + \frac{Q_0}{\rho c_p}(T - T_\infty) \tag{3}$$

$$u\frac{\partial C}{\partial x} + v\frac{\partial C}{\partial y} = D_m\frac{\partial^2 C}{\partial y^2} \tag{4}$$

The boundary conditions for the model are

$$\left.\begin{aligned} u = Dx,\ v = v_w,\ T = T_w,\ C = C_w \quad at\ y = 0 \\ u = 0,\ T = T_\infty,\ C = C_\infty \quad as\ y \to \infty \end{aligned}\right\} \tag{5}$$

where u and v are the velocity components in x and y directions respectively, υ is the kinematic viscosity, g is the acceleration due to gravity, β is the volumetric coefficient of thermal expansion, T and T_∞ are the fluid temperature within the boundary layer and in the free-stream respectively, while C is the concentration of the fluid within the boundary layer, σ is the electric conductivity, B_0 is the uniform magnetic field strength (magnetic induction), ρ is the density of the fluid, κ is the thermal conductivity of the fluid, C_p is the specific heat at constant pressure, Q_0 is the volumetric rate of heat generation/absorption and D_m is the chemical molecular diffusivity, s is a dummy parameter stands for 0, +1, or -1. $D(>0)$ is a constant, v_w is a velocity component at the wall having positive value to indicate suction, T_w is the uniform wall temperature and C_w, C_∞ are the concentration of the fluid at the sheet and far from the sheet respectively. The effect of the second term on the right hand side of equation (2) is due to buoyancy force. If s = 1, the buoyancy force is dominant and the governing equations (1)-(4) reduce to those of natural convection limit. In order to obtain a solution of equations (1)-(4), we introduce the following similarity variables

$$\eta = y\sqrt{\frac{D}{\upsilon}},\ \psi = \sqrt{D\upsilon}\,x\,f(\eta),$$

$$\theta(\eta) = \frac{T - T_\infty}{T_w - T_\infty},\ \phi(\eta) = \frac{C - C_\infty}{C_w - C_\infty} \tag{6}$$

where

$$u = Dx\,f'(\eta),\ v = -\sqrt{D\upsilon}\,f(\eta) \tag{7}$$

where, f, θ and ϕ are the dimensionless velocity, temperature and concentration respectively, and η is the similarity variable. By taking into account the above similarity variables, equations (1)-(4) become

$$f''' + f f'' - (f')^2 - Mf' + \lambda\theta = 0 \quad (8)$$

$$\theta'' + \Pr f\theta' + \Pr Q\theta = 0 \quad (9)$$

$$\phi'' + S_c f\phi' = 0 \quad (10)$$

The last term in equation (8) is due to the buoyancy force and $\lambda = \frac{sg\beta(T_w - T_\infty)}{D^2 x}$ which serves as the buoyancy parameter. The transformed boundary conditions are:

$$\left.\begin{aligned} f' = 1, f = f_w, \theta = 1, \phi = 1 \ \ at \ \ \eta = 0 \\ f' = 0, \theta = 0, \phi = 0 \ \ as \ \ \eta \to \infty \end{aligned}\right\} \quad (11)$$

where $f_w = -\frac{v_w}{\sqrt{D\upsilon}}$ is the suction parameter, $M = \frac{\sigma B_0^2}{\rho D}$ is the magnetic field parameter, $\Pr = \frac{\mu c_p}{\kappa}$ is the Prandtl number, $Q = \frac{Q_0}{\rho c_p D}$ is the heat source/sink parameter, $S_c = \frac{\upsilon}{D_m}$ is the Schmidt number.

Numerical Computation: The numerical solutions of the non-linear differential equation (8)-(10) under the boundary conditions (11) have been performed by applying a shooting method namely Nachtsheim-Swigert (1995) iteration technique (guessing the missing values) along with sixth order Runge-Kutta iteration scheme. We have chosen a step size $\Delta\eta = 0.001$ to satisfy the convergence criterion of 10^{-6} in all cases.

The value of η_∞ was found to each iteration loop by $\eta_\infty = \eta_\infty + \Delta\eta$. The maximum value of η_∞ to each group of parameters f_w, M, Pr, λ, Sc and Q determined when the values of the unknown boundary conditions at $\eta = 0$ not change to successful loop with error less than 10^{-6}. In order to verify the effects of the step size $\Delta\eta$, we ran the code for our model with three different step sizes as $\Delta\eta = 0.01$, $\Delta\eta = 0.005$, $\Delta\eta = 0.001$ and in each case we found excellent agreement among them. The Fig. 2(a), 2(b) and 2(c) show the velocity, temperature and concentration profiles for different step sizes.

RESULT AND DISCUSSION

For the purpose of discussing the results of the flow field represented in the Fig.1, the numerical calculations are presented in the form of non-dimensional velocity,

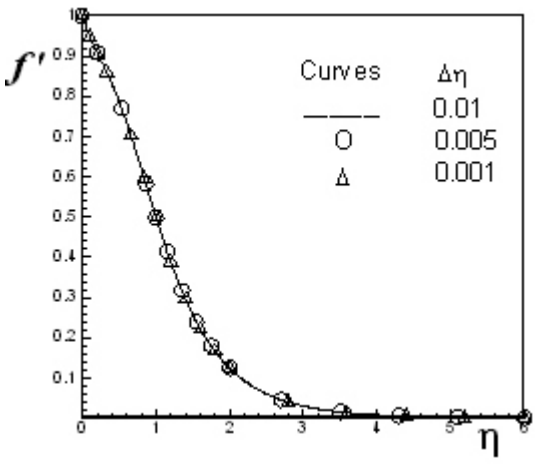

(a)

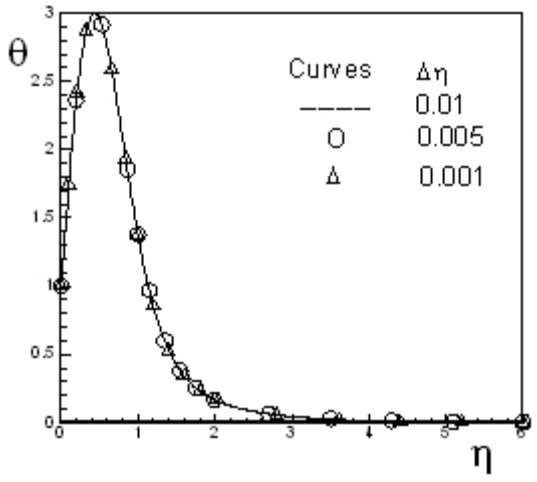

(b)

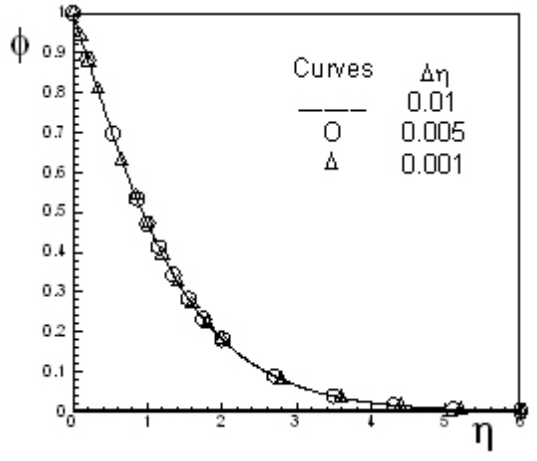

(c)

Fig. 2: Velocity, temperature and concentration profiles for different step size $\Delta\eta$: (a) velocity, (b) temperature and (c) concentration

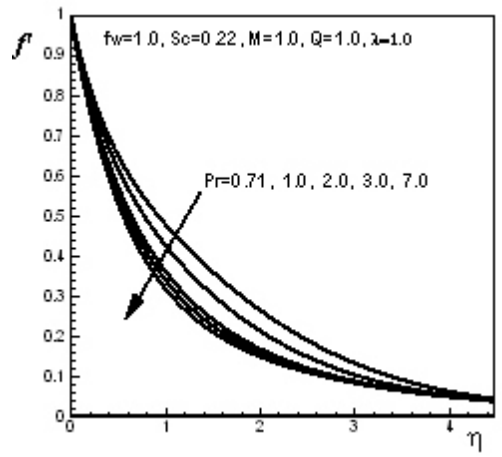

(a)

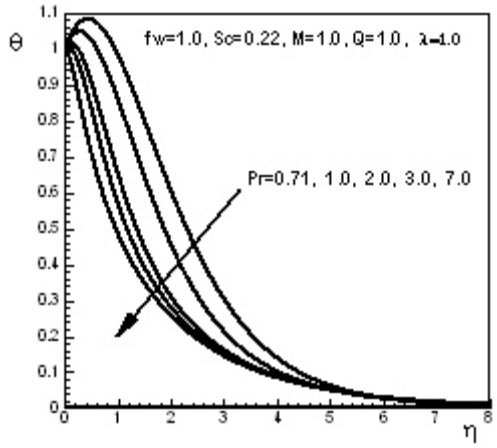

(b)

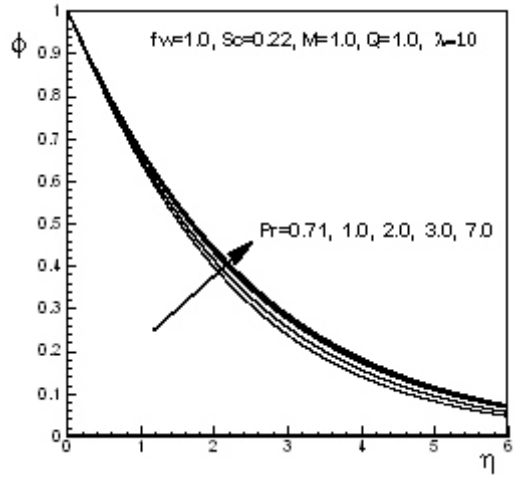

(c)

Fig.3: Velocity, temperature and concentration profiles for different values of *Pr* (a) velocity, (b) temperature and (c) concentration

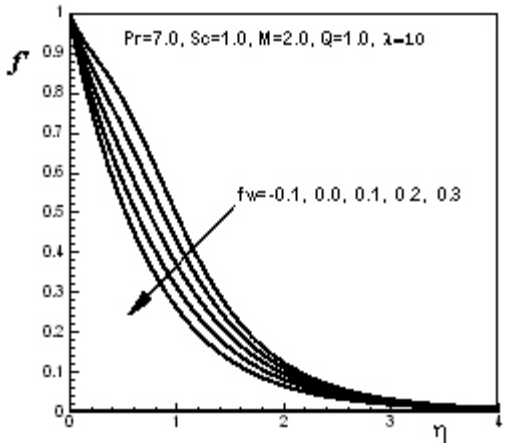

(a)

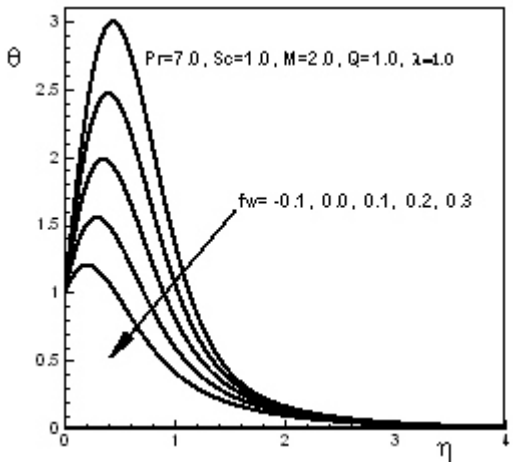

(b)

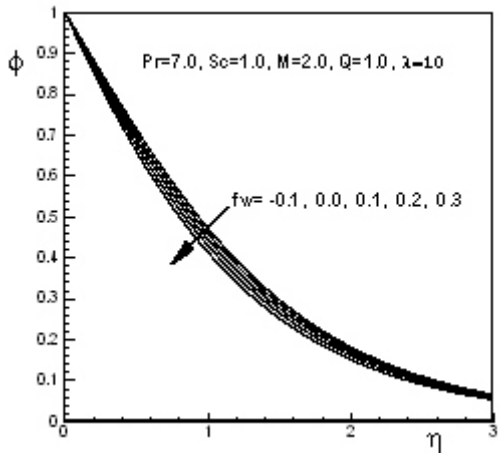

(c)

Fig.4: Velocity, temperature and concentration profiles for different values of f_w, (a) velocity, (b) temperature and (c) concentration

temperature and concentration profiles. Numerical computations have been carried out for different values of the Prandtl number (Pr), Magnetic field parameter (M), Schmidt number (Sc), Heat source/sink parameter (Q) and Suction parameter (f_w). These are chosen arbitrarily where Pr = 0.71 corresponds physically to air at 20°C, Pr = 1.0 corresponds to electrolyte solution such as salt water and Pr = 7.0 corresponds to water and Sc = 0.22, 0.6 and 1.0 corresponds to hydrogen (Sc = 0.22), water vapor (Sc = 0.6) and methanol (Sc = 1.0) respectively at approximate 25°C and 1 atmosphere.

In Fig.3 we have plotted the dimensionless velocity, temperature and concentration profiles showing the effects of the Prandtl number Pr. It can be seen that the velocity f' and θ temperature decrease but the concentration ϕ increases, when the Prandtl number increases. The concentration boundary layer thickness reduces as we increase. The velocity gradient at the surface is negative, which signify that the stretching sheet velocity is higher than the adjacent fluid velocity. The temperature gradient at the surface is decreasing from positive value to negative. The temperature gradient at the surface is zero for pr = 7.44853. That means if we increase pr from 0.71, the stretching sheet gains temperature from the environment but the heat gaining rate decreases, when we reach 7.44853 the heat gaining rate is zero, further increasing of pr heat transfer rate from the stretching sheet increases.

Fig.4 displays the effects of the suction parameter f_w on the velocity, temperature and concentration profiles. We observe that, as we increase suction f_w, the velocity, temperature and concentration decrease monotonically. This figures indicate that, increasing suction enhance the heat and mass transfer coefficient since the boundary layer thickness getting smaller but the temperature and concentration gradient at the stretching sheet getting steeper.

The effects of magnetic field on the dimensionless velocity, temperature and concentration profiles are shown in Fig.5. From Fig.5 (a) we observe that the velocity decreases near the wall and after η = 1.75 starts to increase. This is due to the effect of magnetic field on the stretching sheet. The temperature field increases with the increase of magnetic field as seen in the Fig.5 (b) and we find the increasing effect of concentration as show in Fig.5(c).

From Fig.6 we see that velocity and temperature decrease uniformly with the increase of Schmidt number Sc up to a value about 0.6, which is for water vapor. But when Sc gets large exceeding 0.6, velocity and temperature profiles remain same. Fig.6(c) indicates the concentration profiles showing the effect of Schmidt number Sc. It can be seen that concentration profiles decrease very rapidly and the hydrodynamic, thermal and concentration boundary layer thickness reduce with the increase of Sc.

Fig.7 shows the velocity, temperature and concentration profiles for different values of heat source/sink parameter Q. It is observed that the dim ensionless velocity increases but the concentration

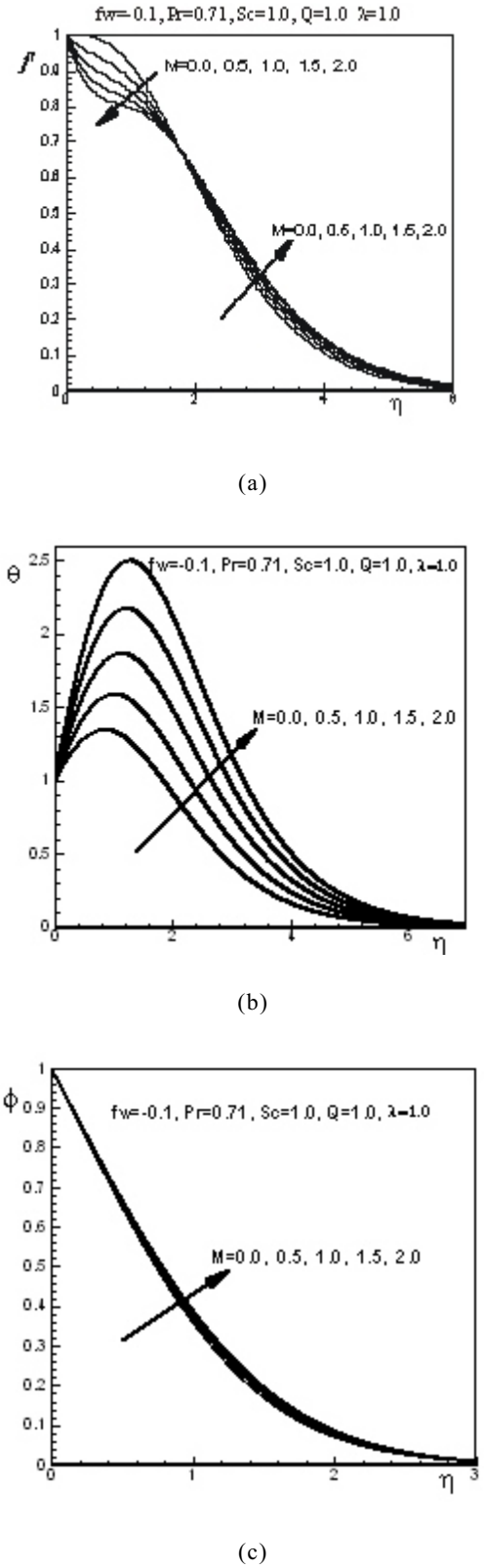

Fig. 5: Velocity, temperature and concentration profiles for different values of M (a) velocity, (b) temperature and (c) concentration

decreases uniformly as the heat source/sink parameter Q increases. It is also observed that as Q increases the temperature increases rapidly and overshoot the stretching sheet temperature. The temperature gradient at the surface is increasing from negative to positive as we increase Q. This means that Q = 0.5 when the temperature is transferred from the sheet, but for increasing, the heat transfer rate is decreasing, when the Q = 0.998873 temperature gradient at the sheet is zero, if we further increase Q, the temperature gradient increases to positive value, that is, the stretching sheet gains temperature from the environment. The hydrodynamic and thermal boundary layers thickness increase but the concentration boundary layer thickness reduces with the increase of Q.

In Fig.8 we have plotted the dimensionless velocity, temperature and concentration profiles showing the effect of buoyancy parameter λ. We see that the velocity increases near the wall and after that starts to decrease from η = 1.6, due to the effect of buoyancy parameter λ on the stretching sheet. The velocity gradient at the surface is positive, which signify that the stretching sheet velocity is smaller than that of the adjacent fluid velocity. The temperature and concentration profiles decrease with the increase of λ. It is clear that as λ increase the thermal boundary layer thickness reduces and also the temperature gradient at the surface decreases from positive value to negative value. Temperature gradient at the surface positive means that heat is transferred from the ambient medium to the sheet. Therefore as we increase λ from 1.0, the sheet initially gains temperature from the environment and after $\lambda = \lambda_{(crt)}$ = 4.5586485, the sheet starts leaving temperature to the ambient medium $\lambda = \lambda_{(crt)}$ = 4.5586485 for zero temperature gradient at the surface. It is also clear that, the velocity gradient at the surface increases from negative to a positive value. The specific critical value of $\lambda = \lambda_{(crt)}$ = 2.4112 is for zero velocity gradient where the surface shear stress is vanished and $\lambda = \lambda_{(crt)}$ = 4.5586485 for zero temperature gradient at the surface.

Finally, the parameters of engineering interest for the present problem are the skin friction coefficient (C_f), the local Nusselt number (Nu_x) and the local Sherwood number (Sh), which indicate physically wall shear stress, local wall heat transfer rate and wall mass transfer rate respectively.

The skin-friction coefficient is given by

$$c_f = \frac{2}{\sqrt{\mathrm{Re}}} f''(0) \tag{12}$$

The local heat transfer coefficient is defined as

$$Nu_x = -\sqrt{\mathrm{Re}}\,\theta'(0) \tag{13}$$

The local Sherwood number (Sh) is obtained as

$$Sh = -\sqrt{\mathrm{Re}}\,\phi'(0) \tag{14}$$

Thus from equations (12) - (14) the values proportional to the skin-friction coefficient, Nusselt number and Sherwood number are $f''(0)$, $-\theta'(0)$ and $-\phi'(0)$ respectively. The numerical values proportional to C_f, Nu_x and Sh, calculated from equations (12) - (14) are shown in Table1- Table 3.

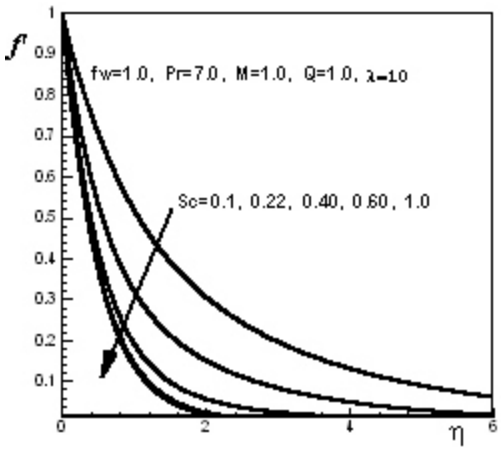

(a)

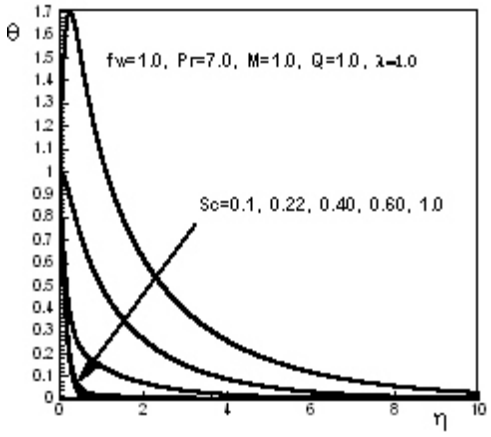

(b)

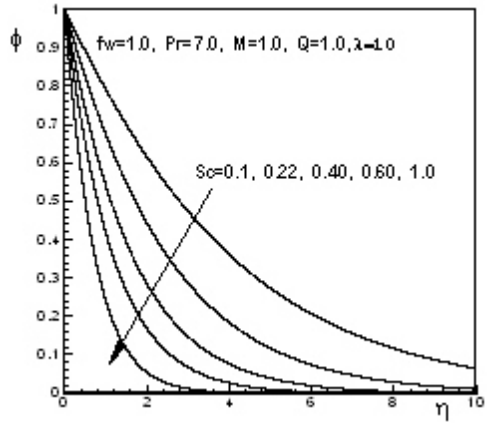

(c)

Fig.6: Velocity, temperature and concentration profiles for different values of (a) velocity, (b) temperature and (c) concentration

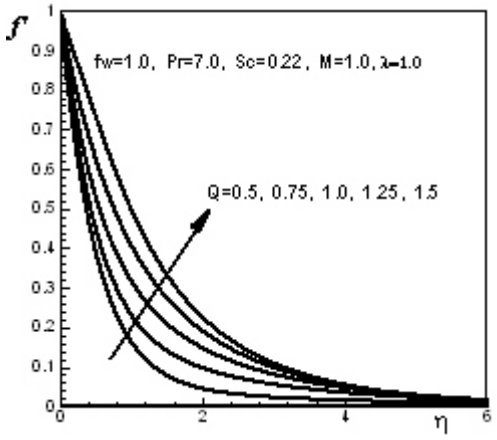

(a)

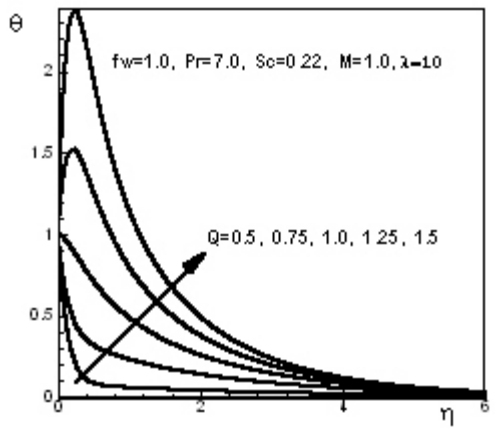

(b)

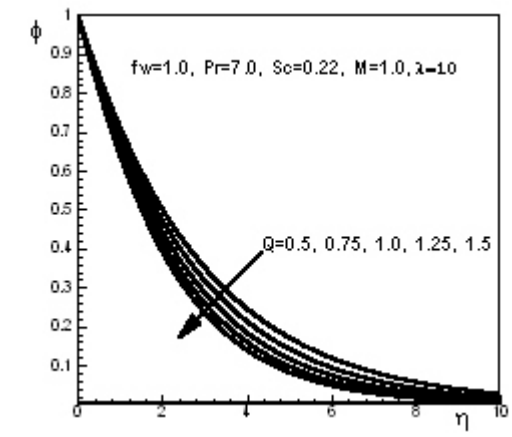

(c)

Fig.7: Velocity, temperature and concentration profiles for different values of *Q*, (a) velocity, (b) temperature and (c) concentration

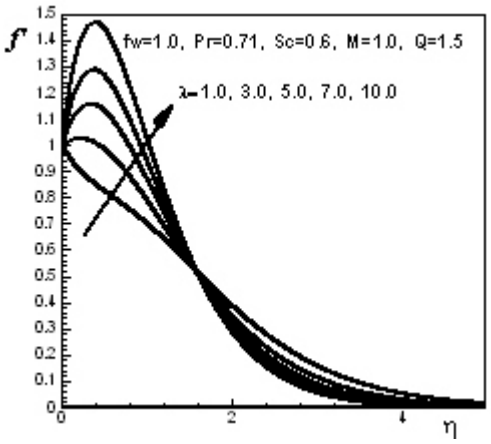

(a)

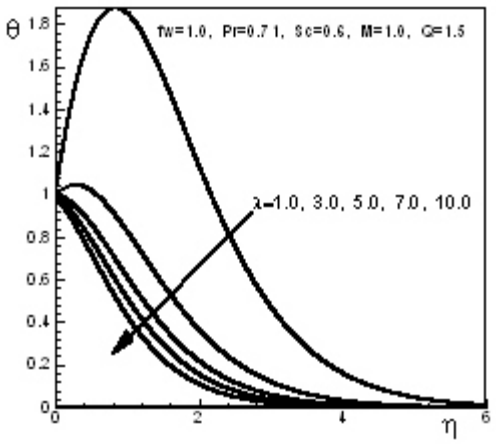

(b)

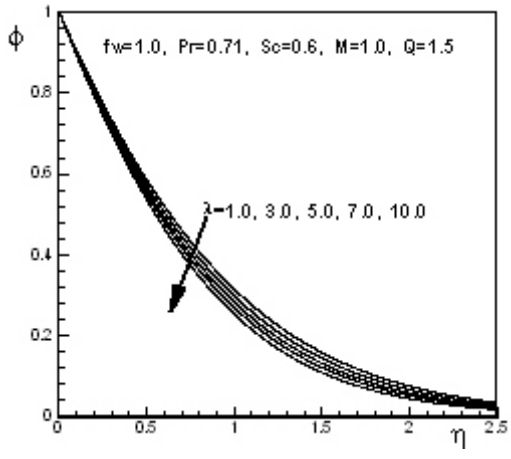

(c)

Fig.8: Velocity, temperature and concentration profiles for different values of, (a) velocity λ, (b) temperature and (c) concentration

Table1: C_f, Nu_x and Sh for different values of Pr, M.

Pr	C_f	Nu_x	Sh	M	C_f	Nu_x	Sh
0.71	-1.0586135	-0.3988216	0.4070962	0.0	0.0088494	-0.7831341	0.7149090
1.0	-1.1387943	-0.3531551	0.3945218	0.5	-0.1914180	-1.0886432	0.6999995
2.0	-1.2533078	-0.2852384	0.3805534	1.0	-0.3692765	-1.4137521	0.6878163
3.0	-1.3011301	-0.2306239	0.3761920	1.5	-0.5308114	-1.7513681	0.6775278
7.0	-1.3671478	-0.0218965	0.3714634	2.0	-0.6795450	-2.0982242	0.6686882

Table2: C_f, Nu_x and Sh for different values of Sc, Q.

Sc	C_f	Nu_x	Sh	Q	C_f	Nu_x	Sh
0.1	-0.8075037	-7.7688333	0.2217558	0.50	-1.8219962	6.6466806	0.3283488
0.22	-1.3671478	-0.0218965	0.3714634	0.75	-1.6384904	4.2397439	0.3495120
0.40	-1.7307807	4.8247070	0.5788442	1.00	-1.3671478	-0.0218965	0.3714634
0.60	-1.8651732	6.5816711	0.8167032	1.25	-1.0213637	-6.4136517	0.3924887
1.0	-1.8832373	6.8165325	1.3007012	1.50	-0.6080686	-15.2103334	0.4123933

Table3: C_f, Nu_x and Sh for different values of f, λ.

f	C_f	Nu_x	Sh	λ	C_f	Nu_x	Sh
-0.1	-0.5977894	-7.6697661	0.5796245	1.00	-0.5832767	-2.2008276	0.9807700
0.0	-0.7834865	-6.7644595	0.6187596	3.00	0.2404924	-0.3366579	1.0132378
0.1	-0.9767769	-5.4931225	0.6610735	5.00	1.0295899	0.0605359	1.0430976
0.2	-1.1719933	-3.9218291	0.7071052	7.00	1.7785432	0.2515683	1.0695051
0.3	-1.3633177	-2.1424364	0.7575198	10.0	2.8371519	0.4195393	1.1036445

CONCLUSION

Heat and mass transfer and also the flow field characteristics of a linearly stretching vertically moving permeable stretching sheet are studied when buoyancy assists the flow which means that the axis points upwards in the direction of stretching the hot surface such that the stretching induced flow and the thermal buoyant flow assist each other. The results show that skin friction coefficient C_f and the Sherwood number Sh decrease with the increase of the Prandtl number Pr. But the Nusselt number Nu_x increases from negative value with the increase of the Prandtl number Pr, that is temperature gradient at the surface is decreasing from positive value. Which means that the stretching sheet is gaining temperature from the ambient but the heat transfer rate is decreasing as we increase Pr. It can be seen from Table1 that C_f, Nu_x and Sh, and decrease monotonically when the magnetic field parameter M increases. We observe from Table2 that the skin friction coefficient C_f decreases rapidly when the Schmidt number Sc increases from 0.0 to about 0.6, but when Schmidt number Sc gets large, skin friction coefficient C_f decreases to 0.0 slowly. Nusselt number Nu_x increases strictly when the Schmidt number Sc increases from 0.0 to about 0.6, but when Schmidt number Sc gets large, Nusselt number Nu_x increases vary slowly. On the other hand Sherwood number Sh increases strictly as the Schmidt number Sc increases. From Table2 we can also make conclusion that C_f and Sh increase with the increase of the heat source parameter Q. On the other hand Nusselt number Nu_x decreases with the increase of Q. As we increase f_w the Nusselt number Nu_x and the Sherwood number Sh increase but skin friction coefficient C_f decrease. It is seen from the Table3 that the skin friction coefficient C_f, Nusselt number Nu_x and the Sherwood number Sh strictly increase as the buoyancy parameter λ increases.

NOMENCLATURE

B_0 Uniform magnetic field strength
Nu_x Local Nusselt number
C Species concentration
Pr Prandtl number
C_w Concentration at the plate
Q Dimensionless heat source parameter
C_∞ Concentration of the fluid far away from the plate
Q_0 Heat source parameter
C_p Specific heat at constant pressure
q_w Local heat flux
C_f Skin friction coefficient
Sc Schmidt number
D_m Molecular diffusivity
Sh Sherwood number
f Dimensionless stream function
T Temperature within the boundary layer
f_w Suction parameter
T_w Temperature of the fluid at the plate
g Acceleration due to gravity
T_∞ Temperature of the fluid far away from the plate
M Magnetic field parameter
u Component of velocity in the -direction
v Component of velocity in the y-direction
ψ Stream function
v_w Suction velocity
λ Buoyancy parameter
x Coordinate along the plate
σ Electric conductivity
y Coordinate normal to the plate
β Coefficient of volume expansion

Greek Symbols

θ Dimensionless temperature
η Similarity parameter
ρ Density of the fluid
ϕ Dimensionless concentration

μ Coefficient of dynamic viscosity
$\Delta\eta$ Step size
υ Coefficient of kinematic viscosity
κ Thermal conductivity

REFERENCES

Ali, M.E., 1995. On thermal boundary layer on a power-law stretched surface with suction or injection, Internat. J. Heat Fluid Flow, 16(4): 280-290.

Anderson, H.I., O.R. Hansen and B. Holmedal, 1994. Diffusion of a chemically reactive species from a stretching sheet, Int. J. Heat Mass Transfer, pp: 37-659.

Anjalidevi, S.P. and R. Kandasamy, 1999. Effects of chemical reaction heat and mass transfer on laminar flow along a semi infinite horizontal plate, Heat Mass Transfer, pp: 35-465.

Anjalidevi, S.P. and R. Kandasamy, 2000. Effects of chemical reaction heat and mass transfer on MHD flow past a semi infinite plate, Z. Angew. Math. Mech., pp: 80-697.

Chen, C.K. and M.I. Char, 1988. Heat transfer of a continuous stretching surface with suction or blowing, J. Math. Ana. Appl., 135: 568-580.

Chin, D.T., 1975. Mass transfer to a continuous moving sheet electrode, J. Electrochem. Soc., pp: 122- 643.

Crane, L. J. , 1970. Zeitschrift Angewandt Mathematik and Physik , pp: 21- 26.

Das, U.N., R.K. Deka and V.M. Soundalgekar, 1994 Effects of mass transfer on flow past an impulsively started infinite vertical plate with constant heat flux and chemical reaction, Forsch. Ingenieurwes, pp: 60-284.

Erickson, L.E., L.T. Fan and V.G. Fox, 1966. Heat and mass transfer on a moving continuous flat plate with suction or injection, Indust. Eng. Chem. Fundamentals, pp: 5-19.

Fox, V.G., L.E. Erickson and L.T. Fan, 1968. Methods for solving the boundary layer equations for moving continuous flat surfaces with suction and injection, AIChE J., 14: 726-736.

Gorla, R.S.R., 1978. Unsteady mass transfer in the boundary layer on a continuous moving sheet electrode, J. Electrochem. Soc., pp: 125- 865.

Griffith, R.M., 1964. Velocity temperature and concentration distributions during fibre spinning, Ind. Eng. Chem. Fundam., pp: 3- 245.

Magyari, E., M.E. Ali and B. Keller, 2001. Heat and mass transfer characteristics of the self-similar boundary-layer flows induced by continuous surface stretched with rapidly decreasing velocities, Heat Mass Transfer, 38: 65-74.

McLeod, J.B. and K.R. Rajagopal, 1987. On the uniqueness of flow of a Navier-Stokes fluid due to a stretching boundary, Arch. Ration. Mech. Anal., pp: 98-386.

Muthucumaraswamy, R. and P. Ganesan, 2000. On impulsive motion of a vertical plate with heat flux and diffusion of chemically reactive species, Forsch. Ingenieurwes, pp: 66-17.

Nachtsheim, P. R. and P. Swigert, 1995. Satisfiction of the asymptotic boundary conditions in numerical solution of the systems of non-linear equations of boundary layer type, NASA TN D-3004.

Raptis, A. and C. Perdikis, 2006. Viscous flow over a non-linearly stretching sheet in the presence of a chemical reaction and magnetic field, Int. J. Non-linear Mechanics, 41: 527-529.

Sakiadis, B.C., 1961. Boundary layer behavior on continuous solid surfaces: I, Boundary-layer equations for two-dimensional and axisymmetric flow, AIChE J., 7(1): 7-28.

Vajravelu, K. and A. Hadjinicolaou, 1997. Convective heat transfer in an electrically conducting fluid at a stretching surface with uniform free stream, Int. J. Engng. Sci., 35(12-13): 1237-1244.